Study of Phospholipid Structure by ^{1}H, ^{13}C, and ^{31}P Dipolar Couplings from Two-Dimensional NMR

M. Hong, K. Schmidt-Rohr, and D. Nanz
Materials Science Division, Lawrence Berkeley Laboratory, and Department of Chemistry, University of California, Berkeley 94720 USA

ABSTRACT Various motionally averaged ^{31}P-^{1}H, ^{13}C-^{1}H, ^{1}H-^{1}H, and ^{31}P-^{13}C dipolar couplings were measured for natural-abundance and unoriented phosphocholine in the L_α phase. The couplings were obtained and assigned by a variety of advanced and partly novel two-dimensional solid-state NMR experiments. Whereas ^{31}P-^{1}H and ^{31}P-^{13}C dipolar couplings provide long-range structural constraints, geminal ^{1}H-^{1}H couplings and the signs of ^{13}C-^{1}H couplings are important new elements in a segmental order-tensor analysis of the lipid headgroup and glycerol backbone. The implications of these measured dipolar couplings for the conformational exchange of the lipid headgroup and the bending of the headgroup from the glycerol backbone are discussed. These dipolar couplings are also analyzed semiquantitatively in terms of the segmental order tensor.

INTRODUCTION

The molecular conformation and dynamics of phospholipids have important implications for the detailed understanding of membrane function, fluidity, composition, and protein-lipid interactions. For two decades, phospholipids have been persistently investigated by ^{2}H NMR (Seelig et al., 1987; Blume et al., 1982; Skarjune and Oldfield, 1979; Seelig and Seelig, 1975), ^{31}P NMR (Smith and Ekiel, 1984; Kohler and Klein, 1976), ^{13}C NMR (Sanders, 1993; Husted et al., 1993; Wittebort et al., 1982), various scattering techniques (Pascher et al., 1987; Pearson and Pascher, 1979), and molecular dynamics simulations (Stouch, 1993; Pastor et al., 1991). Early neutron scattering data indicated, for example, that the headgroups of phospholipids orient roughly perpendicular to the bilayer normal (Seelig et al., 1977), whereas ^{2}H NMR showed that the acyl chain segments experience an increasing motional freedom toward the methyl terminus. Although NMR could in principle provide much more detailed information on the segmental orientation and dynamics of the lipid in the L_α phase, the NMR data available so far do not permit rigorous quantification. A distinct disadvantage of the otherwise succssful ^{2}H NMR approach is that only absolute values of the averaged quadrupolar couplings are obtained (Seelig and Seelig, 1980). The information on the segmental orientation is thus not distinguished from effects of motional amplitude. This is in contrast to the determination of dipolar couplings, where addidtional sign information can be obtained (Hong et al., 1995) to deduce orientational information.

In this paper, we report the concerted application of partly novel two-dimensional (2D) NMR methods to provide additional data on the headgroup and the glycerol backbone structure of phosphatidylcholine (PC, or lecithin) in the L_α phase. Our strategy, which does not require isotopic enrichment of the samples, mainly focuses on the measurement of the magnitude and sign of dipolar couplings and the determination of segmental order parameters in unoriented lipids. We completed our previous measurement of ^{13}C-^{1}H dipolar couplings (Hong et al., 1995) so that the order parameters of most ^{13}C-^{1}H bonds are now determined with their signs. We obtained geminal ^{1}H-^{1}H dipolar couplings, which yield valuable ^{1}H-^{1}H order parameters. Furthermore, we investigated long-range couplings, namely, ^{31}P-^{1}H and ^{13}C-^{31}P dipolar couplings, which have not been measured in pure phosphocholine before. These data will contribute to a more complete understanding of the segmental order of phospholipids.

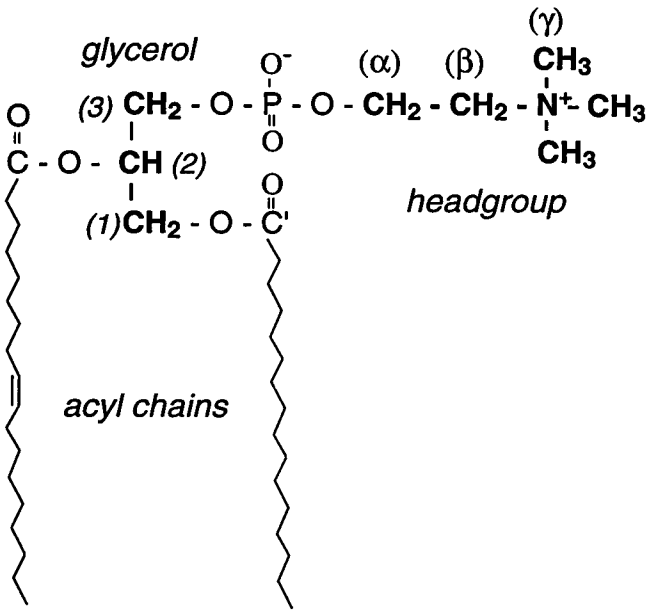

Schematic of lecithin chemical structure

Received for publication 14 April 1995 and in final form 27 July 1995.

Address reprint requests to Dr. Mei Hong, Department of Chemistry, Pine Research Group, University of California-Berkeley, Berkeley, CA 94720. Tel.: 510-642-2094; Fax: 510-486-5744; E-mail: mei@dirac.cchem.berkeley.edu.

The present address of Dr. Schmidt-Rohr is Department of Polymer Science and Engineering, University of Massachusetts, Amherst, MA 01003.

The present address of Dr. Nanz is Organisch-chemisches Institüt, der Universität Zürich, Winter-thurerstrasse 190, CH-8057 Zürich, Switzerland.

0006-3495/95/11/1939/00 $2.00

To provide the necessary NMR background, we summarize some basic NMR properties of lipid bilayers and introduce the 2D NMR pulse sequences used to obtain coupling information. The results will then be presented and discussed in terms of the structural parameters of lecithin.

MATERIALS AND METHODS

Materials

Most experiments were conducted on egg yolk lecithin, i.e., phosphatidylcholine with 16:0 (34%), 18:1 (31%), and 18:2 (18%) acyl chains. The ^{31}P-^{1}H/^{31}P chemical shift correlation experiment was also applied to 16:0–18:1 phosphatidylethanolamine (PE) and sphingomyelin (SPM) to compare with PC. The samples were purchased as powders from Avanti Polar Lipids (Alabaster, AL). The powders were hydrated with D_2O (w/w ratio of ~70:30) and then freeze-thawed with liquid nitrogen to form a uniform aqueous dispersion. Dimyristoylphosphocholine (DMPC) from Sigma (St. Louis, MO), hydrated at 50:50 (w/w), was used in the ^{13}C WISE and the ^{13}C-^{1}H PDLF experiments.

Experimental

The experiments with sample spinnning were carried out on a home-built 7.07 Tesla spectrometer with a Tecmag pulse programmer and data acquisition system. The sample was spun on a Doty Scientific 7-mm spinner in a home-built switching-angle spinning probehead (Eastman et al., 1992) at about 2 kHz. The rotor orientations were controlled by a stepping motor attached to the bottom of the probe and a computerized motor controller with an angular precision of 0.1°. The rotor axis was hopped on and off the magic angle within less than 50 ms. ^{13}C and ^{1}H rf field strengths between 40 kHz and 50 kHz were used. MREV-8 cycle times were 120 μs.

For the static 2D correlation experiments a solution-NMR "inverse" probe on a Bruker AM 400 spectrometer was used. The proton line of H_2O was shimmed to 6 Hz. The PE and SPM samples were heated to 305 K and 320 K, respectively, so that the ^{31}P chemical shift spectra are motionally narrowed. MREV-8 cycle times varied from 180 μs to 200 μs, with ^{1}H 90° pulse lengths of 13 ± 2 μs and short window periods of 3 μs. The MREV-8 scaling factor for these static correlation experiments was experimentally determined to be 0.47 ± 0.04. A Hartman-Hahn match was achieved at field strengths B_1 of about $(2\pi * 17 \text{ kHz})/\gamma$. For the samples measured at 9.4 Tesla, the bilayer directors were found to be oriented preferentially perpendicular to the NMR tube and the field axis, possibly a result of sample rolling before insertion into the 5-mm tube.

Theory

Under biological conditions, lipid molecules in a bilayer exist in the liquid crystalline L_α phase, undergoing fast uniaxial motions around the director, which is the normal of the bilayer. Unless a sample is prepared with special precautions it will exhibit an isotropic distribution of bilayer orientations, which results in inhomogeneously broadened powder spectra. The restricted anisotropic motion of the lipid molecules gives rise to partially averaged interaction tensors that are axially symmetric around the director. Therefore, all averaged NMR interactions have the same orientation dependence with respect to the external field, i.e., they are scaled by a factor $\frac{1}{2}(3\cos^2\theta - 1)$, where θ is the angle between the director and the B_0 field. One consequence of this parallelism of the NMR interactions is the "magic-angle hole" in the cross-polarization (CP) (Pines et al., 1973) ^{31}P spectrum. The vanishing intensity at the isotropic chemical shift frequency of the powder spectrum reflects vanishing ^{31}P-^{1}H dipolar couplings in domains where the bilayer director subtends the magic angle with respect to the external magnetic field. Because of the isotropic distribution of the bilayer orientation, the powder spectrum of a line split by dipolar coupling with a spin of ½ displays two maxima whose separation is the averaged dipolar anisotropy $\bar{\delta}_d$ (if the scalar coupling is disregarded). The spectral narrowing relative to the full splitting δ_d of the corresponding rigid segment contains information about molecular conformation and dynamics. This information is summarized most elegantly in terms of the segmental order tensor **S**, a second-rank tensor defined by

$$S_{ij} = \frac{1}{2}\langle 3\cos\alpha_i\cos\alpha_j - \delta_{ij}\rangle \quad (1)$$

where α_i are the angles between the director and the axes of the segment-fixed frame in which the matrix representation of the order tensor is given (Saupe, 1966). The segmental order tensor relates to the measurable averaged NMR anisotropy parameter $\bar{\delta}$ according to

$$\bar{\delta} = \frac{2}{3}\sum_{i,j} S_{ij}\omega_{ij} \quad (2)$$

where ω_{ij} are the elements of the NMR interaction tensor in the same segment-fixed frame as S_{ij}. For dipolar spin-pair couplings, relation (2) is simplified to

$$\bar{\delta}_d = \frac{\delta_d}{2}[S_{33}(3\cos^2\theta - 1) - (S_{22} - S_{11})\sin^2\theta\cos 2\phi] \quad (3)$$

where θ, ϕ specify the polar coordinates of the internuclear vector in the principal-axis system (PAS) of the order tensor.

According to Eq. 1, the order tensor **S** is traceless ($S_{11} + S_{22} + S_{33} = 0$) and symmetric ($S_{ij} = S_{ji}$), and therefore contains five independent elements. By measuring at least five averaged anisotropies of segment-fixed NMR interactions for each segment, a system of linear equations can be established that allows a complete characterization of the **S** tensor. Once this tensor is known, the averaged anisotropy of any segment-fixed interaction can be predicted according to Eq. 2.

The number of unknowns can be reduced by considering the symmetry of the molecule or by assuming the presence of specific molecular motions. For instance, in most early studies it was assumed that the lipid molecules are rigid and rotate about a molecular axis. This leads to $S_{22} - S_{11} = 0$ and the same S_{33} for all segments. With an assumed value of S_{33}, $\bar{\delta}_d$ provides the orientation of the internuclear vector relative to the molecular rotation axis. The validity of these assumptions, however, has not been proved, and it has been shown that even with such simplifying assumptions the headgroup structure cannot be determined uniquely from the ^{2}H and ^{31}P NMR data (Skarjune and Oldfield, 1979).

In several previous studies of phospholipids, the two ^{2}H quadrupolar couplings of each methylene group have been found to be nearly degenerate, even when their magnitudes were drastically varied, for instance by incorporating electric charges into the lipid bilayers (Scherer and Seelig, 1989). The model that has been proposed to explain this degeneracy is based on a fast conformational exchange between one or several pairs of mirror-symmetric headgroup structures such that the geminal protons effectively interchange (Seelig et al., 1977; Gally et al., 1975). By this exchange, the order tensor of these segments acquires a symmetry plane perpendicular to the H-H vector, which is thus parallel to one principal axis of **S**. The number of unknowns in the order tensor is now reduced to three. Two of these are principal values and one is an angle that orients the principal axis in the symmetry plane.

NMR techniques

In this section, we describe the 2D NMR techniques developed to obtain new segmental and long-range structural constraints, with our focus on the headgroup and glycerol backbone regions of phosphocholine.

Proton-detected local-field NMR

Most of the 2D techniques in this paper employ proton-detected local-field (PDLF) spectroscopy to indirectly detect heteronuclear dipolar couplings

along the ω_1 dimension. The PDLF approach, which is based on earlier work by Weitekamp et al. (1982) and Caravatti et al. (1982), was recently developed as a technique to obtain simplified heteronuclear dipolar spectra of polymers (Nakai and Terao, 1992) and liquid crystals (Schmidt-Rohr et al., 1994). Such PDLF spectra are governed by simple two-spin interactions because the dipolar field is probed at the abundant spins (e.g., ^{1}H) rather than at the rare spin, as in traditional separated local-field experiments. It should be noted that the local fields are probed during the evolution period of the 2D experiments, whereas the signal of the dilute spins is observed in the detection period of the 2D experiment. "Detection" in the term PDLF refers to detection of local fields, not of NMR signals. The two-dimensional PDLF spectrum exhibits the simplified heteronuclear dipolar patterns along the ω_1 dimension, separated by or correlated with a second interaction such as the chemical shift in the ω_2 dimension.

^{31}P-^{1}H heteronuclear coupling

In phospholipds in the L_α phase, the dipolar couplings between the single ^{31}P spin and the many ^{1}H spins in the headgroup and glycerol regions can be measured with the PDLF technique. 2D spectra that correlate ^{31}P-^{1}H Pake patterns with the ^{31}P chemical shift powder pattern are obtained with the pulse sequence of Fig. 1 *a*. During the t_1 period, ^{1}H magnetization effectively evolves under ^{31}P-^{1}H dipolar couplings, because MREV-8 multiple-pulse decoupling removes the proton homonuclear interaction, and two simultaneous 180° pulses on the ^{31}P and ^{1}H spins in the middle of the t_1 period refocus the chemical shifts without affecting the ^{31}P-^{1}H dipolar interaction. The ^{1}H magnetization, modulated by the ^{31}P-^{1}H coupling, is then transferred through cross-polarization to ^{31}P for detection under broad-band ^{1}H decoupling. Because of the parallelism of the motionally averaged interactions (see above), cross sections along either dimension of the 2D spectrum display sharply resolved peaks that are free of inhomogeneous broadening.

^{1}H-^{1}H homonuclear coupling

Geminal proton-proton couplings in the headgroup and glycerol CH_2 moieties could be quantitatively determined by correlating them either with ^{31}P-^{1}H couplings or with ^{1}H chemical shifts. The pulse sequence for the first type is shown in Fig. 1 *b*. In the PDLF evolution period, the ^{1}H magnetization evolves under the ^{31}P-^{1}H dipolar interaction, as both the ^{1}H-^{1}H coupling and the chemical shift interactions are removed. The ^{1}H magnetization is then directly detected in t_2 without any spin manipulation. Since the ^{1}H-^{1}H coupling is by far the strongest interaction experienced by the proton spins, the ω_2 dimension is dominated by the homonuclear couplings. Normally, broad proton lines would have to be expected in ω_2 due to the multiple-spin interactions and the isotropic distribution of bilayer orientations. However, the orientational broadening was avoided by spectral selection of a narrow range of bilayer orientations. This was achieved by cross-polarizing the protons from the ^{31}P spin before the evolution period, with a ^{31}P spin-lock field weaker than the ^{31}P CSA. Because the ^{31}P frequency was set at the maximum of the ^{31}P powder spectrum, mainly bilayers with directors perpendicular to the external field were detected. The selectivity is additionally improved by the "magic-angle hole" at the ^{31}P isotropic chemical shift position in the CP spectrum. The 2D spectra obtained with this technique were found to display little orientational broadening in the homonuclear coupling patterns along the ω_2 dimension.

The ^{31}P-^{1}H/^{1}H-^{1}H correlation spectrum did not provide a definite assignment of the ^{1}H-^{1}H couplings to the corresponding segments. This information could be obtained in part by correlating the ^{1}H-^{1}H couplings with the ^{1}H chemical shift in a modification of the experiment just discussed. Upon removal of the ^{1}H 180° pulse in the evolution period (Fig. 1 *c*) it is now the ^{1}H chemical shift interaction that evolves during t_1 while the ^{31}P-^{1}H couplings are refocused. This experiment was conducted without sample rotation and thus leads to a high resolution in the dipolar dimension, but a low resolution in the chemical shift dimension.

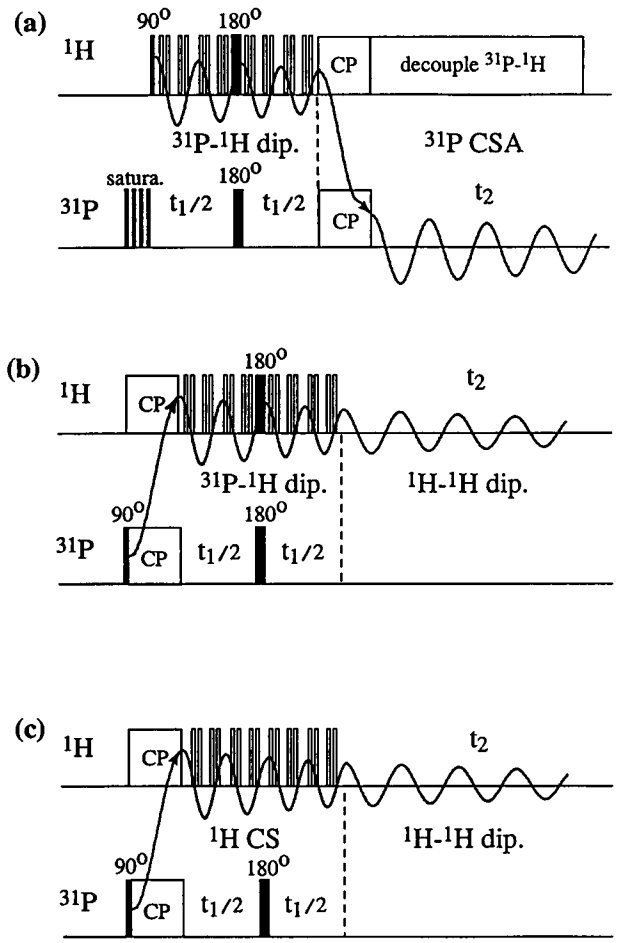

FIGURE 1 NMR pulse sequences used in this work for experiments without sample spinning. (*a*) Correlation of ^{31}P-^{1}H dipolar couplings with ^{31}P chemical shift. In the evolution period, ^{1}H magnetization evolves under the ^{31}P-^{1}H interaction. MREV-8 provides homonuclear decoupling and a pair of 180° pulses refocuses the ^{1}H and ^{31}P chemical shift evolution. Cross-polarization (CP) transfers the ^{1}H magnetization to ^{31}P magnetization, which is detected under proton broad-band decoupling. (*b*) Correlation of ^{31}P-^{1}H couplings with all proton interactions. CP from ^{31}P to ^{1}H selects the protons that couple strongly to the ^{31}P nucleus and the bilayers whose directors are perpendicular to the B_0 field. During the evolution time the ^{1}H magnetization evolves under the ^{31}P-^{1}H dipolar coupling. It is then detected with all local interactions present, which are dominated by the large ^{1}H-^{1}H dipolar couplings. (*c*) Correlation of ^{1}H chemical shifts with ^{1}H-^{1}H couplings. A 180° pulse on the ^{31}P channel is applied in the middle of the evolution period, so that the ^{31}P-^{1}H dipolar coupling is refocused while the ^{1}H chemical shift is retained. The ^{1}H magnetization evolving under the unperturbed Hamiltonian (mainly the ^{1}H-^{1}H coupling) is then detected.

Significantly better chemical shift separation is achieved with sample rotation. The ^{1}H-^{1}H dipolar couplings, scaled by off-magic-angle spinning (OMAS), are correlated with the ^{1}H isotropic chemical shift spectrum under magic-angle spinning (MAS) (Fig. 2 *a*). The ^{1}H lines under MAS are broken into a narrow centerband and spinning sidebands due to the uniaxial motional averaging of the lipid molecules (Forbes et al., 1988; Maricq and Waugh, 1979). Thus, the centerband region exhibits relatively well-resolved isotropic peaks. Proton single-pulse excitation was chosen because the selection of a specific bilayer orientation by selective cross-polarization

from ^{31}P is not possible under sample spinning. As a result, the homonuclear coupling patterns are inhomogeneously broadened. Nonetheless, semiquantitative information on the dipolar couplings of various segments could be obtained from the width of these lines.

Such information was also obtained from experiments where the ^{1}H magnetization was cross-polarized to ^{13}C after the evolution period to correlate the ^{1}H-^{1}H couplings with the isotropic ^{13}C chemical shift. The latter approach, which provides better resolution in the isotropic shift dimension, is similar to the wideline separation (WISE) experiments that have been performed on heterogeneous polymer systems (Schmidt-Rohr et al., 1992).

^{13}C-^{1}H isotropic chemical shift correlation

For the assignment of the couplings in the ^{1}H WISE spectra of lecithin, it proved necessary to completely assign the ^{1}H isotropic chemical shifts. In previous 1D and 2D experiments (Li et al., 1993) the glycerol H1 and H3 sites, which are of specific interest to us, were not resolved. We tackled the problem by a 2D ^{13}C-^{1}H chemical shift correlation experiment (Fig. 2 *b*), in which proton isotropic shifts are correlated with the well-resolved ^{13}C isotropic shifts (Lee and Griffin, 1989). High resolution in the ^{1}H dimension was obtained by measuring out to long evolution times (~13 ms). To avoid sample heating, the ^{13}C-^{1}H J coupling was not decoupled (i.e., no ^{13}C irradiation). Thus the ^{1}H dimension of the spectrum displays $^{1}J(^{13}C,^{1}H)$ splittings centered at the ^{1}H isotropic chemical shifts.

^{13}C-^{31}P heteronuclear coupling

The dipolar couplings between the ^{31}P spin and the nearby ^{13}C spins could be directly observed as splittings of the maxima of the ^{13}C powder patterns. As a result of the parallelism of the motionally averaged interactions in the L_α phase, these splittings correspond directly to the motionally averaged ^{13}C-^{31}P dipolar coupling constants. To reduce the overlap of powder patterns, the ^{13}C spectrum was detected under off-magic-angle spinning with a scaling factor of $P_2(\cos\theta) = -0.3$. Alternatively, the powder overlap can be eliminated by a 2D SAS experiment (Bax et al., 1983; Terao et al., 1984), which separates the ^{13}C anisotropic powder patterns according to the isotropic ^{13}C chemical shifts.

^{13}C-^{1}H dipolar couplings

^{13}C-^{1}H dipolar couplings of directly bonded C-H nuclei provide the same information on bond orientation as ^{2}H quadrupolar couplings. However, although only absolute values of the deuterium couplings have been measured, the signs of the motionally averaged dipolar couplings can be determined in a straightforward manner (Hong et al., 1995) from a pair of 2D PDLF SAS spectra acquired at two different spinning angles. In a previous study, the small C-H couplings of β and γ sites were difficult to measure with high precision due to the inefficient cross-polarization (Hong et al., 1995). Here we extend the CP contact time from the previous 0.5 ms to 2 ms in order to polarize the weakly coupled sites more efficiently. The pulse sequence, with PDLF evolution under ^{13}C-^{1}H dipolar couplings and ^{13}C detection, is shown in Fig. 2 *c*. The sample was spun constantly off the magic angle to avoid the mechanical difficulty of sample hopping. The ^{13}C chemical shifts in the ω_2 dimension were still sufficiently resolved because the OMAS angle θ was chosen such that the scaling factor $P_2(\cos\theta)$ of the anisotropies was quite small (~0.2).

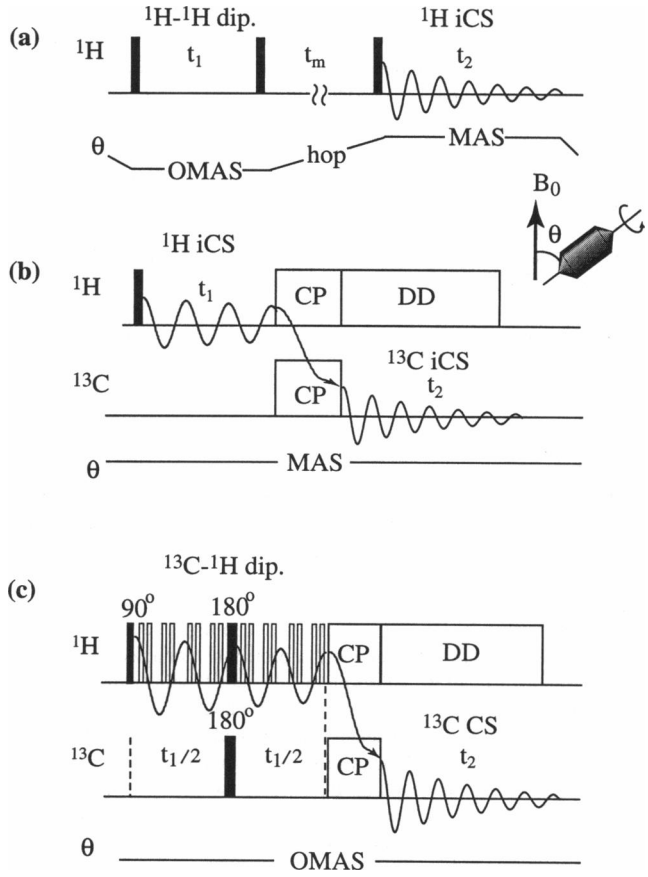

FIGURE 2 NMR pulse sequences of experiments with sample spinning. (*a*) Separation of ^{1}H wideline spectra by isotropic ^{1}H chemical shifts with switching-angle spinning. The sample is spun off the magic angle, i.e., $\theta \neq 54.74°$, in the evolution period and then hopped to the magic angle, $\theta = 54.74°$, for detection. (*b*) Correlation of ^{1}H and ^{13}C isotropic chemical shifts. The sample is constantly spun at the magic angle with respect to the external field. After the evolution period the ^{1}H magnetization is cross-polarized to ^{13}C for detection. (*c*) Correlation of proton-detected ^{13}C-^{1}H dipolar couplings with ^{13}C chemical shifts. In the evolution period, ^{1}H magnetization evolves under the scaled heteronuclear interaction. The cosine-modulated magnetization is then cross-polarized to ^{13}C for detection. The sample is spun off the magic angle throughout the experiment. However, the OMAS scaling factor is small enough to maintain the chemical shift separation in the ω_2 dimension. A CP contact time of 2 ms was chosen to detect weak ^{13}C-^{1}H couplings.

RESULTS

^{31}P-^{1}H dipolar couplings

Fig. 3 *a* shows the 2D spectrum of lecithin that correlates the proton-detected ^{31}P-^{1}H couplings with the ^{31}P chemical shift anisotropy. As explained in the theory section, each inequivalent proton group coupled to the single ^{31}P spin yields a simple doublet in the ω_1 dimension (Schmidt-Rohr et al., 1994). According to theory, these ^{31}P-^{1}H doublets are symmetric with respect to $\omega_1 = 0$. In our experiment they are artificially made so by exclusive detection of the cosine-modulated term in the ω_1 dimension. Additional acquisition of the sine data set, which contained hardly any signal, would have increased the measuring time by nearly a factor of four for the same signal-to-noise ratio, and therefore was not conducted. The ω_2 dimension of the spectrum shows the ^{31}P chemical shift powder pattern after cross-polarization from ^{1}H, with a distinct "magic-angle hole" at the isotropic chemical shift. The values of the ^{31}P-^{1}H dipolar couplings can be extracted most accurately from a cross-section taken

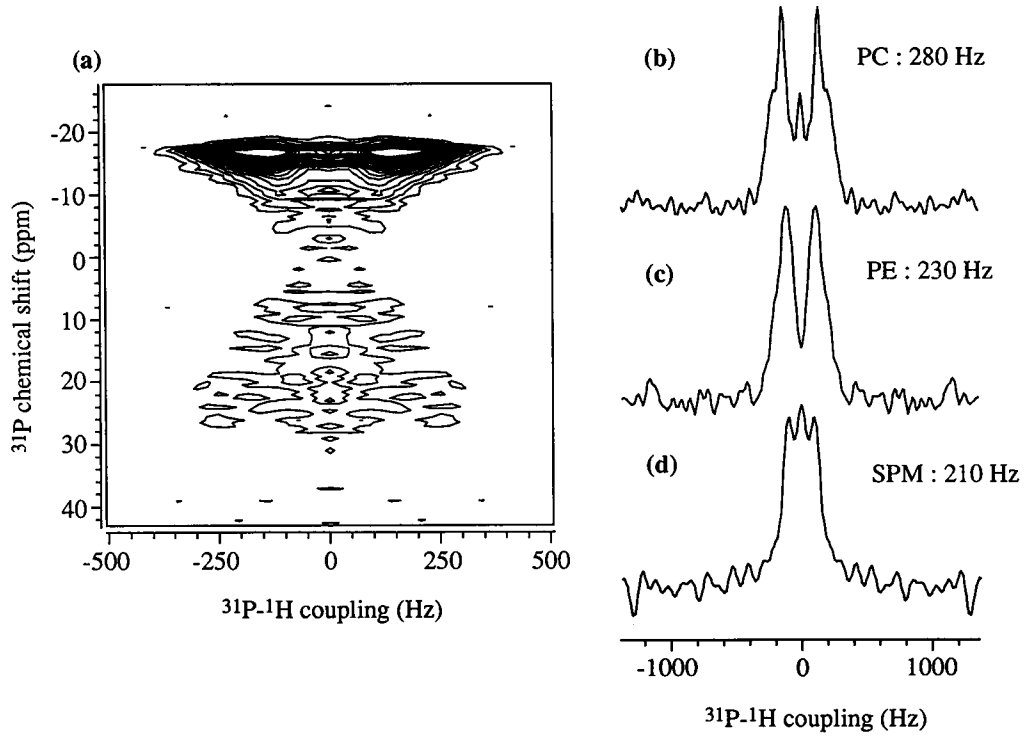

FIGURE 3 ^{31}P-^{1}H couplings in L_α lecithin correlated with the ^{31}P chemical shift anisotropy. (*a*) The 2D spectrum exhibits intensities in two opposite triangles, with zero intensity at the isotropic chemical shift as a result of the "magic-angle-hole" effect (see Theory). The ^{31}P-^{1}H dipolar powder pattern in the ω_1 dimension is symmetric because only the cosine-modulated term was measured in t_1. The MREV-8 scaling factor was experimentally determined to be 0.47 ± 0.04. (*b–d*) Cross sections along the ^{31}P-^{1}H coupling dimension for (*b*) PC, (*c*) PE, and (*d*) SPM, taken at the maximum of the ^{31}P powder pattern in the respective 2D spectra.

at the maximum of the ^{31}P powder pattern. This dipolar spectrum, which results from those bilayers with directors normal to the external magnetic field, exhibits a doublet with a splitting of ~280 Hz (Fig. 3 *b*) for lecithin.

The experiment was also applied to PE at 305 K and SPM at 320 K. Their ^{31}P-^{1}H couplings are compared with those of lecithin in Fig. 3, *b–d*. The SPM spectrum exhibits a reduced splitting of about 210 Hz, compared to 280 Hz for lecithin. The relative intensity of the central frequency and the general lineshape are markedly different from those of the lecithin spectrum. This suggests that the headgroups of lecithin and SPM have quite different conformations, in spite of their similar chemical structures and the ^{31}P chemical shift patterns. The ^{31}P-^{1}H couplings in PE (~230 Hz) are found to be intermediate between those of lecithin and SPM. In addition, the PE spectrum exhibits no zero-frequency peak, indicating that the central-frequency peaks in lecithin and SPM spectra arise from weak unresolved ^{31}P-^{1}H couplings.

The ^{31}P-^{1}H couplings are long-range interactions that are affected by internuclear distances, orientations of the internuclear vectors with respect to the director, and internal molecular motions. In particular, all protons are at least three bonds away from the ^{31}P nucleus, so that the ^{31}P-^{1}H distances depend on one or more torsional angles. Thus, the ^{31}P-^{1}H couplings provide long-range constraints on structural models of the headgroup and the glycerol backbone, but cannot be used for characterizing the order tensor of a specific segment.

Individual ^{31}P-^{1}H doublets superposed in the cross sections of Fig. 3 *b* can be experimentally separated by additional NMR interactions, namely ^{1}H-^{1}H couplings and ^{1}H chemical shifts. To avoid a 3D experiment, one can remove the ^{31}P chemical shift dimension by applying a spectroscopic selection of the 90° orientation of the bilayers. Such a selection was obtained by positioning the ^{31}P rf frequency at the maximum of the ^{31}P powder spectrum, as discussed before.

When the ^{31}P-^{1}H interaction is correlated with the ^{1}H-^{1}H interaction, two major ^{31}P-^{1}H doublets are resolved, with the bigger splitting correlating with the larger ^{1}H-^{1}H coupling in the other dimension (Fig. 4 *a*). The magnitudes of the ^{31}P-^{1}H couplings are found to be 300 ± 30 Hz and 210 ± 20 Hz, as shown in two cross sections along the ^{31}P-^{1}H dimension (Fig. 4 *b*). Tentatively, these couplings can be assigned to the glycerol C3 and the headgroup C_α protons, because they are closest to the phosphate unit. This assignment will be corroborated below.

^{1}H-^{1}H homonuclear dipolar couplings

In the ^{31}P-^{1}H/^{1}H-^{1}H correlation spectrum, two ^{1}H-^{1}H doublets with splittings of 6.8 ± 0.4 kHz and 1.9 ± 0.4 kHz are observed, as shown in Fig. 4 *c*.

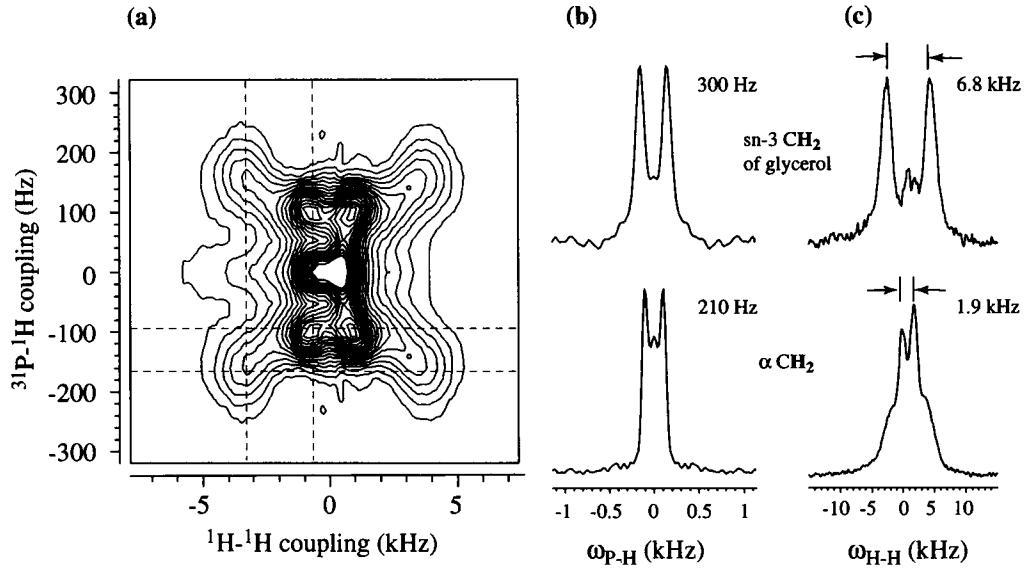

FIGURE 4 Correlation of the ^{31}P-^{1}H couplings in lecithin with the ^{1}H-^{1}H dipolar couplings. (*a*) 2D spectrum. The ω_{P-H} dimension is symmetric because only the cosine-modulated term was measured in t_1. (*b*) Two cross sections along the ω_{P-H} dimension, showing ^{31}P-^{1}H couplings of 300 Hz and 210 Hz. (*c*) The corresponding cross sections along the ω_{H-H} dimension, exhibiting ^{1}H-^{1}H couplings of 6.8 kHz and 1.9 kHz, respectively. The larger ^{1}H-^{1}H and ^{31}P-^{1}H couplings can be assigned to the C3 site of the glycerol backbone, and the smaller couplings are due to the C_α group (see text).

To assign these two couplings, the ^{1}H-^{1}H dipolar couplings were correlated with the ^{1}H chemical shift by using the pulse sequence of Fig. 1 *c*. Because the experiment was conducted without sample rotation, the ^{1}H chemical shift of the different molecular sites exhibit anisotropy broadening and thus make the separation of the ^{1}H-^{1}H coupling patterns incomplete. However, the ^{1}H chemical shifts of interest overlap only partially. This can be inferred from the values of the isotropic and anisotropic components of the ^{1}H chemical shifts. The ^{1}H isotropic shifts of lecithin are precisely known from a ^{13}C-^{1}H MAS heteronuclear correlation spectrum (Fig. 5). The H2 resonance at 5.3 ppm and the H_β resonance near 3.8 ppm are well separated from the H3 and H_α signals near 4.2 ppm. The ^{1}H chemical shift anisotropies are expected to be narrowed by the lipid motion from their full width of 6 ppm to ~1.5 ppm (glycerol protons) or less (~0.4 ppm for headgroup protons). Thus in the 2D shift-coupling correlation spectrum (not shown), the chemical shift-resolved ^{1}H-^{1}H couplings at 4.2 ppm (Fig. 6 *a*) must represent the H3 and H_α signals. The two splittings were found to be 6.2 ± 0.7 kHz and 1.8 ± 0.4 kHz, consistent with those of Fig. 4. This confirms our previous assignment of the two splittings in the ^{31}P-^{1}H/^{1}H-^{1}H spectrum to the protons of the C3 and C_α sites. A reliable discrimination between H3 and H_α is not possible here because of the presence of chemical shift anisotropies, but can be achieved by other experiments. Fig. 6 *b* shows the ω_1 cross section of the 2D spectrum at 5.3 ppm, corresponding to the glycerol C2 segment. It exhibits a hump without a resolved splitting, consistent with the presence of only one proton at this site.

The next question to be addressed is determining which dipolar coupling results from the glycerol H3 protons and which from the headgroup H_α protons. We expected the smaller ^{1}H-^{1}H splitting to be associated with the H_α protons, because they are closer to the mobile end of the headgroup. A WISE-SAS experiment that separates ^{1}H-^{1}H couplings according to the *isotropic* ^{1}H chemical shift indeed con-

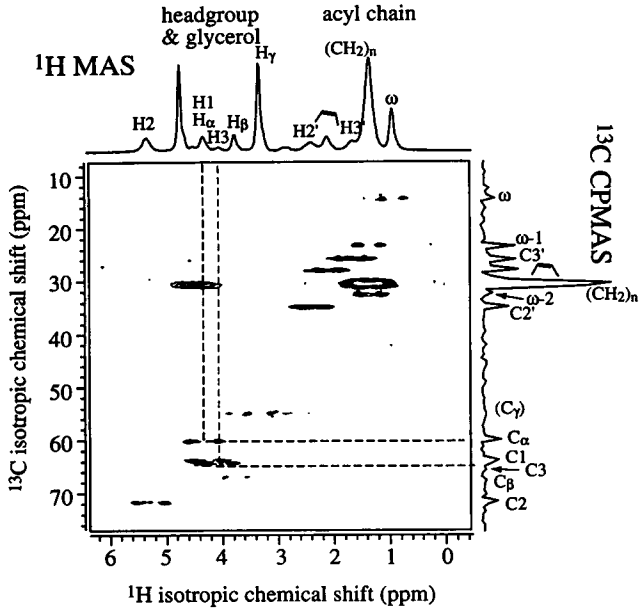

FIGURE 5 ^{13}C-^{1}H heteronuclear MAS correlation spectrum of L_α lecithin. By the well-resolved and fully assigned ^{13}C isotropic chemical shifts (Husted et al., 1993), the H3, H1, and H_α proton resonances in the glycerol and headgroup regions are unambiguously determined. Because of heteronuclear C-H J-couplings, each ^{1}H signal is split into a doublet whose center is the ^{1}H isotropic chemical shift. The 1D MAS spectra of ^{1}H and ^{13}C are shown along the two dimensions for comparison. The sample was spun at 2 kHz.

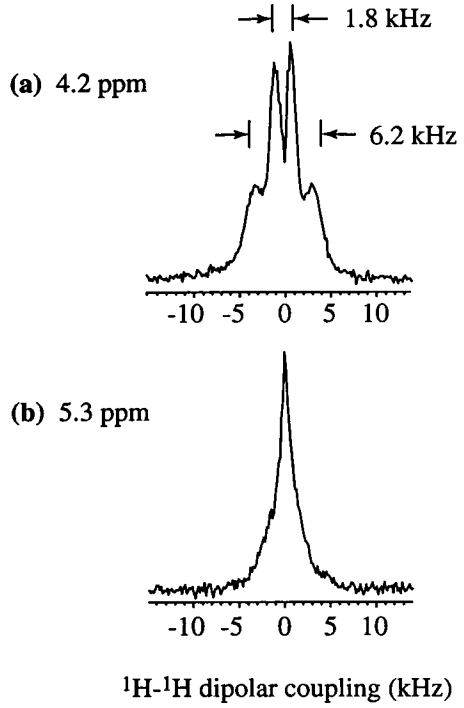

FIGURE 6 Cross sections of the 2D spectrum of L_α lecithin correlating ^{1}H-^{1}H couplings with ^{1}H chemical shifts under the static condition. (*a*) ^{1}H-^{1}H couplings of the H_α and H3 sites, taken from the slice with ^{1}H chemical shift of 4.2 ppm. (*b*) The cross section of the glycerol H2 site, at a ^{1}H chemical shift of 5.3 ppm. No splitting can be observed for this methyne site with a single proton.

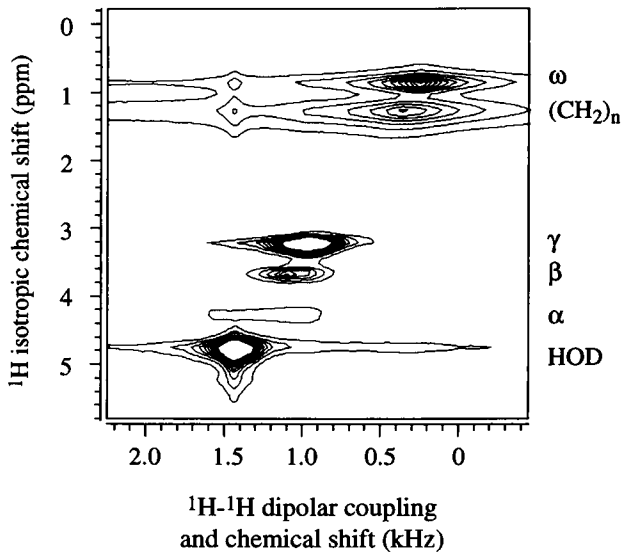

FIGURE 7 ^{1}H WISE-SAS spectrum of L_α lecithin. The homonuclear coupling dimension is scaled by $P_2(\cos 69°) = -0.3$. The widths of the proton lines suggest the magnitudes of the homonuclear couplings. The α-proton resonance has a width of ~2.5 kHz, whereas the resonance of the glycerol H3 protons is too broad to be observed. Several spin diffusion peaks can be seen, for instance, between the signals of aliphatic protons and HOD. The spinning speed was 2 kHz.

firmed this hypothesis. From the C-H heteronuclear correlation spectrum (Fig. 5) it can be seen that the H_α and H3 isotropic shifts are separated by only 0.3 ppm, with the H_α signal being more downfield and closer to the HOD peak. According to this assignment, the ^{1}H WISE spectrum (Fig. 7) with an OMAS scaling factor of $P_2 = -0.3$ demonstrates that the H_α resonance has a linewidth of about 2.1 kHz, whereas the signals of the glycerol H3 protons are too broad to be seen in the spectrum and show fast decays in the t_1 time domain. As a result, the larger ^{1}H-^{1}H coupling in Figs. 4 *c* and 6 *a* must be assigned to the H3 protons, and the smaller coupling is due to the H_α protons.

The above assignment of the geminal ^{1}H-^{1}H couplings was corroborated by a ^{13}C WISE experiment, which separates the proton widelines by the well-resolved ^{13}C isotropic chemical shift. Fig. 8 shows a stack plot of the ^{13}C-WISE spectrum of DMPC, in which the α and β sites exhibit smaller couplings (~1.6 kHz) than all three glycerol sites, whose signals are so broad that they are hardly observable.

The reason why the WISE technique produced broad ^{1}H dipolar lines instead of resolved ^{1}H-^{1}H dipolar doublets is that no specific bilayer orientation was selected. On the other hand, the presence of relatively well-resolved ^{1}H-^{1}H doublets in the spectra of Figs. 3 and 4 is not only a result of the orientation selection. These doublets indicate an upper limit of 1 kHz to the nongeminal ^{1}H-^{1}H couplings.

This rather small value is consistent with conclusions drawn from ^{2}H NMR. The fast conformational exchange between mirror-symmetric headgroup structures reduces the couplings between protons of different segments, while the ^{1}H-^{1}H couplings between geminal protons are invariant to the exchange. Therefore, in the headgroup and backbone

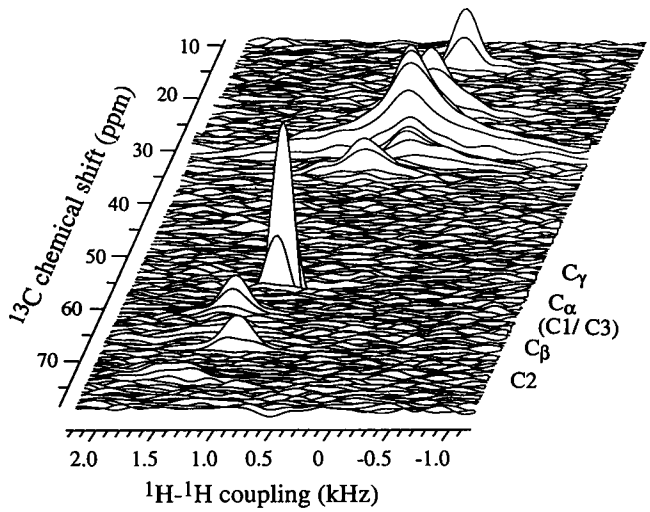

FIGURE 8 WISE spectrum, with ^{13}C detection, of L_α DMPC, taken at an OMAS scaling factor of $P_2(\cos 47°) = +0.2$ and a spinning speed of 2 kHz. Hopping was omitted because the ^{13}C chemical shifts of different sites are sufficiently separated in the ω_2 dimension at this angle. The widths of the proton lines indicate the strengths of homonuclear couplings. The α-protons have a much narrower ^{1}H dipolar line than the H1 and H3 protons of the glycerol backbone.

regions, the geminal ^{1}H-^{1}H couplings are much stronger than the nongeminal ^{1}H-^{1}H couplings, and a simple doublet splitting results for each segment.

The shape of ^{1}H dipolar powder spectra of molecules undergoing uniaxial motions has been simulated by Bloom et al. (1977). There, the Hamiltonian was taken to consist of a geminal ^{1}H-^{1}H coupling that gives rise to a dipolar doublet, and lumped nongeminal ^{1}H-^{1}H couplings that produce Gaussian broadening. Both types of couplings scale as $P_2(\cos\theta)$ with the angle θ between the bilayer director and the B_0 field. For very small nongeminal ^{1}H-^{1}H couplings, a Pake pattern is obtained. It was found that the larger the relative size of the broadening function to the geminal ^{1}H-^{1}H splitting, the more the spectral lineshape becomes logarithmic, or super-Lorentzian. Such a logarithmic line exhibits a sharp cusp at the center, corresponding to molecules oriented and rotating at the magic angle with respect to the B_0 field. Thus the half-width of such a super-Lorentzian line has little meaning, because it strongly depends on the ratio of geminal and nongeminal ^{1}H-^{1}H couplings and on the intrinsic width of the signal from the molecules at the magic angle. In the case of our ^{1}H WISE spectra, however, only the relative widths of the lines must be considered, because we only need a qualitative assignment of the resolved geminal ^{1}H-^{1}H splittings in the WISE spectra. From Fig. 4, the coupling strength of H3 can certainly be identified as larger than the H_α and H_β couplings, and the H_β coupling is slightly smaller than that of H_α.

^{13}C-^{31}P dipolar couplings

Similar to the ^{31}P-^{1}H couplings, the ^{13}C-^{31}P dipolar couplings provide another type of long-range structural constraints for the conformation of the headgroup and backbone of lecithin. These couplings were reported previously (Sanders, 1993; Sanders and Schwonek, 1992) for DMPC oriented in detergent matrices, in which case extrapolation was necessary to obtain ^{13}C-^{31}P couplings for the pure DMPC. In the present study, we obtained the ^{13}C-^{31}P couplings in pure and unoriented lecithin by a simple off-magic-angle spinning experiment. It gives rise to a ^{13}C spectrum (Fig. 9 *a*) in which the scaled chemical shift powder patterns of C_α and C2 are split by their dipolar interactions with the ^{31}P spin. The size of the splitting corresponds to the P_2-scaled dipolar coupling constant. The sample was spun at 43°, corresponding to a scaling factor of $P_2(\cos\theta) = +0.3$. The scaled ^{13}C CSAs range from −5 ppm (C_1) to +3 ppm (C_α) for the headgroup and backbone segments. The full coupling strengths of C2 and C_α to ^{31}P were found to be 155 ± 15 Hz. Since C3 is closer to the ^{31}P spin than C2, a splitting was also expected at the C3 site. However, the C3 powder pattern overlaps with those of C_β and C_1 and could not be observed in the 1D spectrum. To resolve more ^{13}C-^{31}P dipolar couplings, a 2D SAS experiment that separates the ^{13}C CSA patterns according to the isotropic shift of each site was done. Fig. 9, *c–e*, displays

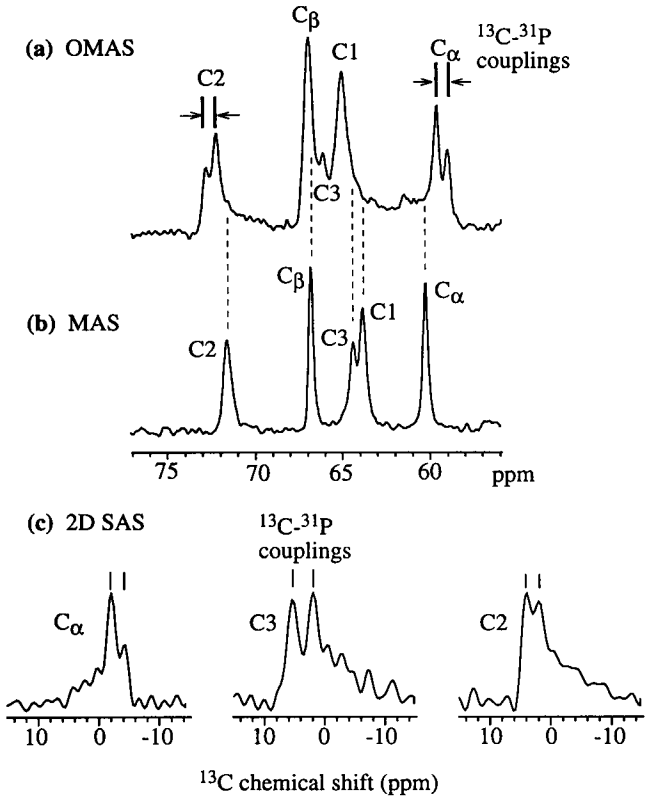

FIGURE 9 ^{13}C-^{31}P dipolar couplings in lecithin. (*a*) ^{13}C OMAS spectrum of the headgroup and glycerol backbone sites, with $P_2(\cos 43°) = +0.3$. The ^{13}C-^{31}P splittings are resolved for C2 and C_α sites. (*b*) The corresponding ^{13}C MAS spectrum for comparison. (*c*) Cross sections from a 2D SAS chemical shift spectrum of lecithin, displaying the ^{13}C-^{31}P couplings in the chemical shift powder patterns of the C_α, C3, and C2 sites, respectively.

the cross sections from the 2D SAS spectrum. They correspond to the C_α, C3, and C2 sites of lecithin. C_α and C2 exhibit clear dipolar splittings of 168 Hz and 144 Hz, respectively, and the C3 carbon has the largest dipolar coupling of 264 Hz.

In principle, the averaged ^{13}C CSAs can serve as important structural constraints on the local conformation of the lipid. However, their use requires precise knowledge of the orientations of the CSA tensors in the molecular segments, which still await determination.

^{13}C-^{1}H dipolar couplings

The signs and magnitudes of weak C-H dipolar couplings were measured with the pulse sequence of Fig. 2 *c*. The 2D C-H PDLF spectra of DMPC in the headgroup and glycerol regions, obtained with $P_2 = \pm 0.2$ in both time domains, is shown in Fig. 10. The spectra show clear C_β and Cγ signals. From the difference of the splittings in the two spectra, the C_β-H dipolar coupling is found to be +175 Hz, whereas the Cγ-H coupling is −110 Hz. The resulting magnitudes of the C-H bond order parameters are in good agreement with ^{2}H NMR results for fully hydrated bilayers. The significant

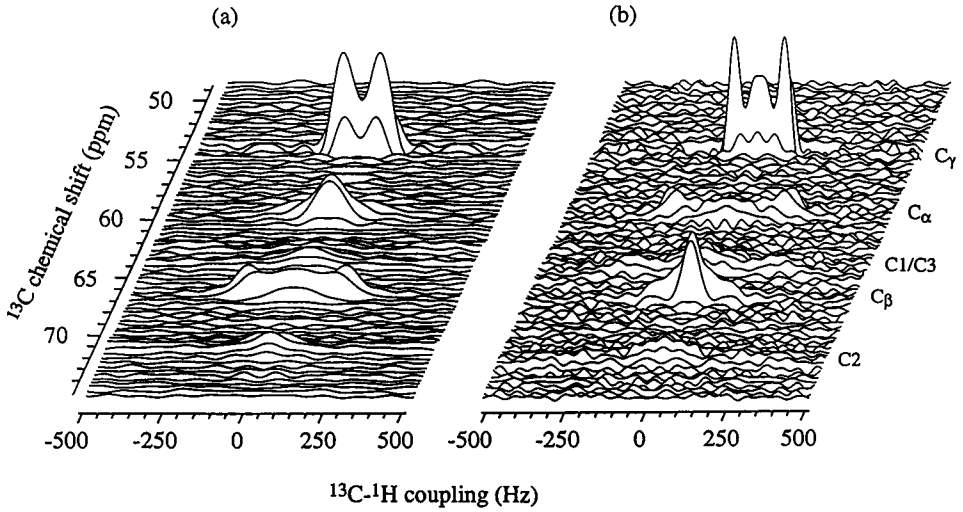

FIGURE 10 2D PDLF spectra, without sample hopping, correlating the ^{13}C-^{1}H couplings with the ^{13}C chemical shift for DMPC in the L_α phase. Only the headgroup and glycerol regions are shown. (*a*) $P_2(\cos 63°) = -0.2$. (*b*) $P_2(\cos 47°) = +0.2$. The weak C-H dipolar couplings of the C_γ and C_β sites can be observed with sufficient sensitivity because of the long CP contact time, which was 2 ms for these spectra. The correlation of the heteronuclear powder spectra with the scaled chemical-shift anisotropies produces characteristic line shapes. Note that the patterns observed for the C_α and C_β sites at opposite P_2 values are similar, because their dipolar couplings have similar magnitudes but opposite signs. Measuring times were 8 and 10 h, respectively.

deviations of the C_α-H and C_β-H dipolar couplings obtained from our previous experiments (Hong et al., 1995) from the current values are most likely due to the different hydration levels of the samples. This can be concluded based on a careful ^{2}H NMR study of the hydration dependence of the headgroup C-H order parameters (Bechinger and Seelig, 1991).

From the P_2 dependence of the splittings in the two spectra, it can be concluded that the γ-methyl groups have a positive C-H order parameter, whereas the C_β-H bonds have a negative one. The present spectra show higher resolution in the dipolar dimension than our previous spectra (Hong et al., 1995), because the dipolar powder broadening is partially removed by "spreading out" the chemical shift frequencies of each site in the ^{13}C dimension as a result of off-magic-angle spinning in that dimension.

So far the C-H couplings of double-bond segments in the acyl chains have not been discussed. Seelig and Waespe-Sarcevic (1978) have measured the ^{2}H quadrupolar splittings in the double bonds and examined their dependence on the *cis* and *trans* conformations. They obtained C-D bond order parameters of ± 0.102 and ± 0.019 for the C9 and C10 sites of the *cis*-9-oleic acid chain. From the PDLF spectrum of lecithin taken with the spinning angle of 63° ($P_2 = -0.2$), we resolved three C-H couplings in the double-bond region (Fig. 11). The two splittings at 130.2 ppm are assigned to the C9 and C13 segments (Husted et al., 1993), where C13 is part of the second double bond in the 9,12-linoleic acid chains of lecithin, and the small splitting at 128.2 ppm corresponds to the C10 site. From two PDLF experiments conducted at different spinning angles, the averaged C-H couplings are found to be +2.1 kHz for the C9 site and +0.83 kHz for the C10 site, corresponding to bond order parameters of -0.09 and -0.036, respectively. The C-H coupling for the C10 site could not be obtained because of its low resolution in the $P_2 = +0.2$ spectrum (not shown).

DISCUSSION

To summarize our findings of the various kinds of dipolar couplings in lecithin, Table 1 lists the H-H, C-H, C-P, and P-H dipolar couplings for the six headgroup and glycerol backbone sites that are of most interest to us. Two types of couplings, C-H and C-P, can be compared with existing data from the literature.

Several of the couplings measured strongly support the notion of an interchange of the geminal protons' C-H vector orientations in the headgroup region, as suggested by the persistent approximate degeneracy of the ^{2}H couplings of geminal deuterons in the headgroup. In our data, we find the expected degeneracy of the two C-H dipolar couplings in each CH_2 group. Additionally, we have established from the 2D PDLF spectra that not only their magnitudes, but also their signs are the same. Similarly, only one P-H coupling is observed for each of the C3 and C_α methylene groups.

A further corroboration of the C-H interchange is provided by the geminal ^{1}H-^{1}H couplings. A motional process interchanging the geminal protons' C-H vector orientations does not affect the geminal protons' ^{1}H-^{1}H internuclear vector, but it partially averages intersegmental ^{1}H-^{1}H couplings. We have found that the geminal ^{1}H-^{1}H couplings dominate by more than a factor of 4 over the nongeminal ones. By contrast, rigid headgroup

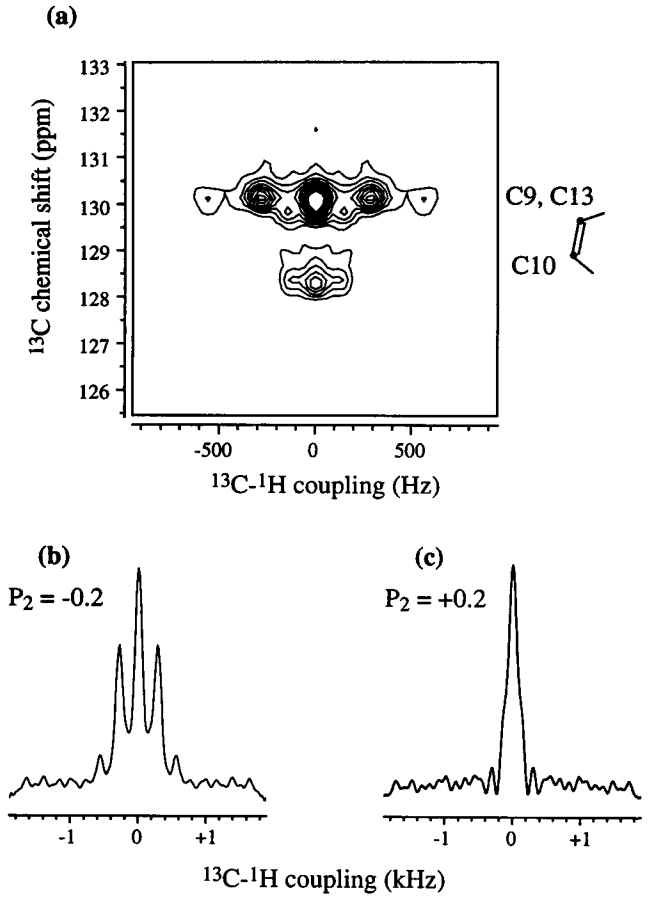

FIGURE 11 Measurement of ^{13}C-^{1}H couplings in the double-bond region of lecithin by the 2D PDLF technique combined with SAS. The sample was spun at 63° during the evolution time so that the dipolar couplings are scaled by $P_2(\cos 63°) = -0.2$. (*a*) The 2D spectrum exhibits two splittings at 130.2 ppm, which are assigned to the C9 and C13 sites. According to the ^{2}H NMR data of Seelig et al. (1978), the C9-H9 coupling corresponds to the larger splitting. The splitting at 128.2 ppm is assigned to the C10 segment. The cross section at 130.2 ppm is shown for both (*b*) and (*c*) . All ^{13}C-^{1}H couplings, including that of the C9 site, are significantly smaller at 47° than at 63°.

conformations found in phosphocholine crystals and used in a simple model with rotation around the molecular long axis exhibit comparable geminal and nongeminal couplings.

Our data, in terms of the magnitude and resolution of the geminal ^{1}H-^{1}H couplings, strongly indicate that the C3 glycerol site participates in the C-H exchange process, while the degeneracy of its ^{2}H couplings was originally explained in terms of a special C2-C3 bond orientation (Seelig et al., 1977). According to that model, the H-H internuclear vector would be perpendicular to the rotation axis, so that the coupling would be scaled by a factor of $-\frac{1}{2}$, and by a molecular order parameter of 0.66 (Seelig et al., 1977). The magnitude of the expected H-H coupling would then amount to more than 10.3 kHz, disagreeing significantly with the 6.6 kHz found experimentally in our study. Conversely, assuming a molecular order parameter of 0.66 and molecular rotation, the measured H-H coupling would correspond to an angle of 68° or 44° between the rotation axis and the H-H vector, deviating significantly from 90°. The magnitude of the H-H order parameter in C3 is calculated to be 0.2 ± 0.02.

Although most P-C couplings are truly long range, the P-C_α and P-C3 couplings are actually fixed by the P-O-C bond angles and bond lengths, which are known from the x-ray structure. From these data we calculate the magnitudes of the P-C_α and P-C3 order parameters to be 0.23 ± 2 and 0.38 ± 0.04, respectively. This makes the P-C3 order parameter the largest order parameter measured in phosphocholine to date. The large P-C3 and P-C2 couplings, as well as the negative signs of the glycerol C-H bond order parameters, are consistent with the notion that the glycerol backbone and its extension to the phosphate unit are roughly parallel to the bilayer normal.

It is interesting to note that C_α, which is one bond closer to the ^{31}P spin than the C2 carbon of the glycerol backbone, has a C-P coupling magnitude comparable to that of the C2 carbon. This indicates that the orientation of the C_α-P vector with respect to the bilayer normal is quite different from that of the C2-P vector, and that the C_α-P vector has a significantly smaller $\langle P_2(\cos\theta)\rangle$ than the C2-P vector. This is consistent with the bend of the phosphocholine headgroup from the glycerol backbone and the acyl chains (Seelig et al., 1977; Büldt et al., 1978).

Our measurement of the signs of the C-H bond order parameters in the double-bond region of the spectrum prompts a reexamination of a previous calculation of segmental order tensors (Seelig and Waespe-Sarcevic, 1978), which was based on two ^{2}H quadrupolar couplings and one order parameter from infrared dichroism. By a sequence of arguments, it was concluded in that study that the signs of the couplings must be negative for the C9 and positive for the C10 site, in contrast to our results of C-H bond order parameters of −0.09 and −0.036, respectively. However, several problems are encountered upon closer examination of the mentioned calculations. It was implicitly assumed that the order tensor **S** in the segment-fixed coordinate system has vanishing off-diagonal elements where the corresponding elements of the NMR interaction tensor are zero. The basis for this assumption is not clear. It may have resulted from the belief that the order tensor possesses the symmetry of the segment, which is not warranted if that symmetry is not shared by the whole molecule. A second problem concerns the exclusion of several possible order tensors based on the questionable assertion that the asymmetry parameter of the segmental order tensor must be very small because of the uniaxiality of the averaged interaction tensors in the lipid. This notion can be disproved by calculating the segmental order tensors for any simple model involving internally flexible molecules. A good example is provided by the pseudo-mirror-image pair exchange model with fast molecular rotation, first proposed by Seelig et al. (1977). With a calculation completely analogous to the two-site exchange problem in ^{2}H NMR, it demonstrates that

TABLE 1 Dipolar couplings and order parameters of the headgroup and glycerol backbone segments in lecithin

Site	^1H ω_i (ppm)	S_{C-H} (dipolar coupling)*	S_{C-H}‡ (^2H $\Delta\nu$)	ω_{HH} (kHz)	ω_{C-P} (Hz)	ω_{C-P}§ (Hz)	ω_{P-H} (Hz)
γ	3.32	+0.005 ± 0.005	±0.009	0.53 ± 0.1	ND	<15	ND
β	3.77	−0.04 ± 0.015	±0.04	1.6 ± 0.3	ND	58 ± 15	ND
α	4.33	+0.04 ± 0.015	±0.05	1.9 ± 0.3	168 ± 15	131 ± 20	210 ± 20
3	4.05	−0.185 ± 0.025	±0.22	6.8 ± 0.4	264 ± 20	219 ± 30	300 ± 30
2	5.37	−0.16 ± 0.04	±0.19	ND	144 ± 15	141 ± 20	ND
1	4.33	−0.12 ± 0.04	±0.16	ND	ND	62 ± 15	ND

*The order parameters are derived from C-H dipolar couplings measured here and in previous studies (Hong et al., 1995). The order parameter is defined as the ratio of the motionally averaged NMR coupling to the rigid limit coupling. The rigid limit C-H coupling for directly bonded C-H with r_{CH} = 1.1A is 22.7 kHz.

‡C-H order parameters were also obtained from ^2H quadrupolar couplings measured by Gally et al. (1975) and Seelig et al. (1977). The rigid limit ^2H coupling constant is 127.5 kHz.

§These C-P dipolar couplings were estimated (Sanders, 1993) by extrapolating the C-P couplings obtained for DMPC macroscopically oriented in various detergent matrices.

ND, not determined.

the asymmetry parameter of the segmental order tensor can have any value between 0 and 1.

As for our measured C-H couplings in the double-bond region, since we do not yet have five motionally averaged segment-fixed couplings, a valid segmental order tensor analysis must be deferred until more couplings are available.

For the headgroup, the single deuterium and C-H dipolar splitting observed for the three CH_3 groups in the $N(CH_3)_3$ moiety strongly suggests that a fast motion with at least C_3 symmetry occurs around the C_β-N bond. Taking the C_β-N-C_γ and N-C_β-H bond angles of 113° and 107° from the x-ray structure of crystalline phosphocholines, we can then deduce that the C_β-N bond order parameter has a value of +0.1 ± 0.02, with the positive sign being determined in our PDLF experiment.

Thus we know three segment-fixed order parameters for the C_β methylene group: the C-H and C-N bond order parameters of −0.04 and +0.1, respectively, and the magnitude of 0.05 of the geminal H-H order parameter. Three experimental values should be sufficient for characterizing the order tensor of the β segment, taking into account the degeneracy of the C-H directions. However, because the sign of the H-H coupling is not known we cannot discriminate between two possible solutions. One possible set of principal values is (0.12 ± 0.02, −0.05 ± 0.01, −0.07 ± 0.02), the other (−0.22 ± 0.03, 0.05 ± 0.01, 0.17 ± 0.03). The latter principal values are significantly larger than the order parameters measured, which is a reminder that it is not possible to argue, based on a few small order parameters, that the order tensor principal values must be small or that the segment is more mobile than others with larger couplings.

To complete the order tensor analysis, a few more segment-fixed order parameters must be determined. These may be obtained from intersegmental dipolar C-H couplings or from chemical shift anisotropies. To convert the latter into useful information, the rigid-limit chemical shift tensors must be determined. Work along these lines is in progress.

CONCLUSIONS AND OUTLOOK

We have shown that many structure-dependent NMR dipolar couplings can be measured in phospholipids by a variety of 2D NMR techniques. For the first time, we determined the magnitudes of H-H and P-H dipolar couplings as well as the signs of most C-H bond order parameters in lecithin. We have discussed how the short-range couplings can be elegantly summarized in terms of segmental order tensors, showing that five independent experimental couplings are required per segment in the most general case. Short- and long-range interactions combined put important constraints on the lipid headgroup structure, providing stringent tests for computer simulations or structural models of phosphocholine. Work is in progress to complete the order tensor analysis by including further C-H couplings and chemical shift anisotropies. The 2D NMR techniques presented here will be applied to other phospholipids such as sphingomyelin and phosphatidylethanolamine, where we expect to identify common structural features as well as possibly biologically relevant conformational differences.

This work was supported by the Director, Office of Energy Research, Office of Basic Energy Sciences, Materials Science Division of the U.S. Department of Energy under contract no. DE-AC03-76SF00098. We are grateful to Professor Alexander Pines for his advice and encouragement of this work. K.S.R. acknowledges a fellowship from the BASF AG and the German National Scholarship Foundation. D.N. thanks the Swiss National Science Foundation for a fellowship.

REFERENCES

Ahlstrom, P., and H. J. C. Berendsen. 1993. A molecular dynamics study of lecithin monolayers. *J. Phys. Chem.* 97:13691–13702.

Bax, A., N. M. Szeverenyi, and G. E. Maciel. 1983. Chemical shift anisotropy in powdered solids studied by 2D FT NMR with flipping of the spinning axis. *J. Magn. Reson. Imaging.* 55:494–497.

Bechinger, B., and J. Seelig. 1991. Conformational changes of the phosphatidylcholine headgroup due to membrane dehydration: a ^2H-NMR study. *Chem. Phys. Lipids.* 58:1–5.

Bloom, M., E. E. Burnell, S. B. W. Roeder, and M. I. Valic. 1977. Nuclear magnetic resonance lineshapes in lyotropic liquid crystals and related systems. *J. Chem. Phys.* 66:3012–3020.

Blume, A., D. M. Rice, R. J. Wittebort, and R. G. Griffin. 1982. Molecular dynamics and conformation in the gel and liquid-crystalline phases of phosphatidylethanolamine bilayers. *Biochemistry.* 21:6220–6230.

Büldt, G., H. U. Gally, J. Seelig, and G. Zaccai. 1978. Neutron diffraction studies on selectively deuterated phospholipid bilayers. *Nature.* 271: 182–184.

Caravatti, P., G. Bodenhausen, and R. R. Ernst. 1982. Heteronuclear solid-state correlation spectroscopy. *Chem. Phys. Lett.* 89:363–367.

Eastman, M. A., P. J. Grandinetti, Y. K. Lee, and A. Pines. 1992. Double-tuned hopping-coil probe for dynamic-angle-spinning NMR. *J. Magn. Reson. Imaging.* 98:333–341.

Ernst, R. R., G. Bodenhausen, and A. Wokaun. 1987. Principles of Nuclear Magnetic Resonance in One and Two Dimensions. Clarendon Press, Oxford.

Forbes, J., C. Husted, and E. Oldfield. 1988. High-field, high-resolution proton MAS NMR studies of gel and liquid crystalline lipid bilayers and the effect of cholesterol. *J. Am. Chem. Soc.* 110:1059–1065.

Gally, H., W. Niederberger, and J. Seelig. 1975. Conformation and motion of the choline head group in bilayers of dipalmitoyl-3-sn-phosphatidylcholine. *Biochemistry.* 14:3647–3652.

Hong, M., and K. Schmidt-Rohr. 1995. Distinct NMR for sign determination of C-H dipolar couplings. *J. Magn. Reson. Imaging.* in press.

Hong, M., K. Schmidt-Rohr, and A. Pines. 1995. NMR measurement of signs and magnitudes of C-H dipolar couplings in lecithin. *J. Am. Chem. Soc.* 117:3310–3311.

Husted, C., B. Montez, C. Le, M. A. Moscarello, and E. Oldfield. 1993. Carbon-13 "magic-angle" sample-spinning nuclear magnetic resonance studies of human myelin, and model membrane systems. *Magn. Reson. Med.* 29:168–178.

Kohler, S. J., and M. P. Klein. 1976. ^{31}P nuclear magnetic resonance chemical shielding tensors of phosphorylethanolamine, lecithin, and related compounds: applications to head-group motion in model membranes. *Biochemistry.* 15:968–973.

Lee, C. W. B., and R. G. Griffin. 1989. Two-dimensional ^{1}H/^{13}C heteronuclear chemical shift correlation spectroscopy of lipid bilayers. *Biophys. J.* 55:355–358.

Li, K., C. A. Tihal, M. Guo, and R. E. Stark. 1993. Multinuclear and magic-angle spinning NMR investigations of molecular organization in phospholipid-triglyceride aqueous dispersions. *Biochemistry.* 32: 9926–9935.

Maricq, M. M., and J. S. Waugh. 1979. NMR in rotating solids. *J. Chem. Phys.* 70:3300–3316.

Nakai, T., and T. Terao. 1992. Measurement of heteronuclar dipolar powder patterns due only to directly bonded couplings. *Magn. Reson. Chem.* 30:42–44.

Pascher, I., S. Sundell, K. Harlos, and H. Eibl. 1987. Conformation and packing properties of membrane lipids: the crystal structure of DMPG. *Biochim. Biophys. Acta.* 896:77–88.

Pastor, R. W., R. M. Venable, and M. Karplus. 1991. Model for the structure of the lipid bilayer. *Proc. Natl. Acad. Sci. USA.* 88:892–896.

Pearson, R. H., and I. Pascher. 1979. The molecular structure of lecithin dihydrate. *Nature.* 281:499–501.

Pines, A., M. G. Gibby, and J. S. Waugh. 1973. Proton-enhanced NMR of dilute spins in solids. *J. Chem. Phys.* 39:569–590

Sanders, C. R., II. 1993. Solid state ^{13}C NMR of unlabelled phosphatidylcholine bilayers: spectral assignments and measurement of carbon-phosphorus dipolar couplings and ^{13}C chemical shift anisotropies. *Biophys. J.* 64:171–181.

Sanders, C. R., II, and J. P. Schwonek. 1992. Characterization of magnetically orientable bilayers in mixtures of DHPC and DMPC by solid state NMR. *Biochemistry.* 31:8898–8905.

Saupe, A. 1966. The average orientation of solute molecules in nematic liquid crystals by proton magnetic resonance measurements and orientation dependent intermolecular forces. *Mol. Cryst.* 1:527–540.

Scherer, P. G., and J. Seelig. 1989. Electric-charge effects on phospholipid headgroups-phosphatidylcholine in mixtures with cationic and anionic amphiphiles. *Biochemistry.* 28:7723–7728.

Schmidt-Rohr, K., J. Clauss, and H. W. Spiess. 1992. Correlation of structure, mobility, and morphological information in heterogeneous polymer materials by 2-dimensional wideline-separation NMR spectroscopy. *Macromolecules.* 25:3273–3277.

Schmidt-Rohr, K., D. Nanz, L. Emsley, and A. Pines. 1994. NMR measurement of resolved dipole couplings in liquid crystals and lipids. *J. Phys. Chem.* 98:6668–6670.

Seelig, A., and J. Seelig. 1975. Bilayers of dipalmitoyl-3-*sn*-phosphatidylcholine confirmational differences between the fatty acyl chain. *Biochim. Biophys. Acta.* 406:1–5.

Seelig, J., H.-U. Gally, and R. Wohlgemuth. 1977. Orientation and flexibility of the choline head group in phosphatidylcholine bilayers. *Biochim. Biophys. Acta.* 467:109–119.

Seelig, J., P. M. Macdonald, and P. G. Scherer. 1987. Phospholipid head groups as sensors of electric charge in membranes. *Biochemistry.* 26: 7535–7541.

Seelig, J., and A. Seelig. 1980. Lipid conformation in model membranes and biological membranes. *Q. Rev. Biophys.* 13:19–61.

Seelig, J., and N. Waespe-Sarcevic. 1978. Molecular order in cis and trans unsaturated phospholipid bilayers. *Biochemistry.* 17:3310–3315.

Skarjune, R., and E. Oldfield. 1979. Physical studies of cell surface and cell membrane structure determination of phospholipid head group organization by deuterium and phosphorus nuclear magnetic resonance spectroscopy. *Biochemistry.* 18:5903–5909.

Smith, I. C. P., and I. H. Ekiel. 1984. Phosphorous-31 NMR: Principles and Applications. I. C. Gorenstein, editor.

Stouch, T. R. 1993. Lipid membrane structure and dynamics studied by all-atom molecular dynamics simulations of hydrated phospholipid bilayers. *Mol. Simul.* 10:335–362.

Terao, T., T. Fujii, T. Onodera, and A. Saika. 1984. Switching-angle sample-spinning NMR spectroscopy for powder-pattern-resolved 2D spectra: measurement of ^{13}C chemical-shift anisotropies in powdered 3,4-dimethoxybenzaldehyde. *Chem. Phys. Lett.* 107:145–148.

Weitekamp, D. P., J. R. Garbow, and A. Pines. 1982. Determination of dipole coupling constants using heteronuclear multiple quantum NMR. *J. Chem. Phys.* 77:2870–2883.

Wittebort, R. J., A. Blume, T. Huang, S. K. D. Gupta, and R. G. Griffin. 1982. Carbon-13 nuclear magnetic resonance investigations of phase transitions and phase equilibria in pure and mixed phospholipid bilayers. *Biochemistry.* 21:3487–3502.